Available online at www.sciencedirect.com
SCIENCE DIRECT®

PERGAMON

International Journal of Heat and Mass Transfer 46 (2003) 2629–2636

International Journal of HEAT and MASS TRANSFER

www.elsevier.com/locate/ijhmt

The onset of convective instability in the thermal entrance region of plane Poiseuille flow heated uniformly from below

Min Chan Kim [a,*], Tae Joon Chung [b], Chang Kyun Choi [b]

[a] Department of Chemical Engineering, Cheju National University, Cheju 690-756, South Korea
[b] School of Chemical Engineering, Seoul National University, Seoul 151-744, South Korea

Received 5 August 2002; received in revised form 12 December 2002

Abstract

The onset condition of regular longitudinal vortex rolls in the thermal entrance region of plane Poiseuille flow heated from below is analyzed. Under propagation theory the stability equations are produced self-similarly, based on scale analysis. The onset position of secondary flow, which represents the starting point of mixed convection, is predicted as a function of the Prandtl number, Reynolds number and Rayleigh number. As expected, the critical position moves upstream as the Rayleigh number increases and an increase in Reynolds number makes the system more stable. The present predictions compare favorably with existing experimental data of water and air.

Keywords: Buoyancy-driven instability; Plane Poiseuille flow; Constant flux heating; Longitudinal vortex rolls; Propagation theory

1. Introduction

It is well-known that a fluid layer becomes unstable when buoyancy forces overcome dissipative ones caused by viscosity and thermal conductivity. The convective motion driven by buoyancy forces has been analyzed extensively since Bénard's [1] systematic experiments and Lord Rayleigh's [2] theoretical analysis were reported. Similarly to Rayleigh–Bénard convection, secondary motion in forms of longitudinal vortex rolls driven by buoyancy forces can set in under forced convection. This roll-type instability has been studied extensively in connection with wide engineering applications such as heat exchangers, electroplating, and chemical vapor deposition [3]. Most of these processes involve nonlinear, developing temperature or concentration profiles and therefore, it becomes an important problem to predict when or where the buoyancy-driven motion sets in.

In thermally and hydrodynamically fully-developed, plane Poiseuille flow Gage and Reid [4] showed that a longitudinal vortex roll is a most preferred instability mode except the case of extremely small Reynolds numbers and its critical condition is exactly the same as that in Rayleigh–Bénard convection. But in the thermal entrance region the basic temperature profile becomes nonlinear and thermally developing in the main flow direction. In this connection, Hwang and Cheng [5], Lee and Hwang [6] and Kim et al. [7] conducted stability analysis on the plane Poiseuille flow heated isothermally from below. The last two results agree favorably with the experimental results of Hwang and Liu [8], Kamotani and Ostrach [9] and Kamotani et al. [10].

For the thermal entrance region of plane Poiseuille flow heated from below with uniform heat flux Incropera and his colleagues [11–17] investigated mixed convection phenomena experimentally and numerically by considering various effects, such as the aspect ratio and boundary conditions. They showed that the onset position of thermal instability is independent of the upper

* Corresponding author. Tel.: +82-64-754-3685; fax: +82-64-755-3670.
E-mail address: mckim@cheju.ac.kr (M.C. Kim).

0017-9310/03/$ - see front matter
doi:10.1016/S0017-9310(03)00037-1

Nomenclature

a	dimensionless wave number
d	fluid layer thickness
Gz	Graetz number, dPe/X
k	thermal conductivity
Nu	Nusselt number, $q_w d/(k\Delta T)$
P	pressure
p	dimensionless pressure disturbance
Pe	Péclet number, $U_{av}d/\alpha$
Pr	Prandtl number, ν/α
q_w	bottom wall heat flux
Ra_q	Rayleigh number, $g\beta q_w d^4/(k\alpha\nu)$
Re	Reynolds number, $U_{av}d/\nu$
T	temperature
(U, V, W)	velocities in Cartesian coordinates
(u, v, w)	dimensionless velocity disturbances in Cartesian coordinates
(X, Y, Z)	Cartesian coordinates
(x, y, z)	dimensionless Cartesian coordinates

Greek symbols

α	thermal diffusivity
Δ_T	thermal boundary-layer thickness
δ_T	dimensionless thermal boundary-layer thickness
ζ	dimensionless similarity variable, $z/x^{1/3}$
θ	dimensionless temperature disturbance, $g\beta d^3 T_1/(\alpha\nu)$
θ_0	dimensionless basic temperature, $k(T_0 - T_i)/(q_w d)$
λ	wavelength of vortex roll
σ	temporal growth rate
ν	kinematic viscosity
τ	dimensionless time

Subscripts

i	inlet conditions
0	basic quantities
1	perturbation quantities
c	critical conditions

Superscript

$*$	transformed quantities

boundary condition. They determined the onset position of instability by flow visualization and heat transfer measurement and showed that the onset position from flow visualization is shorter than that from heat transfer measurement at a given Rayleigh number. Recently Ozsunar et al. [18] conducted experiments that the onset position of instability depends on the aspect ratio and the onset position of instability is delayed with decreasing the aspect ratio for a given Rayleigh number.

To analyze the onset of regular vortex rolls in forced convection flow propagation theory was applied to typical channel flows [7,19]. This theory employs the thermal boundary-layer thickness as a length scaling factor and the linearized equations are transformed into self-similar forms. The critical conditions are obtained under the principle of the exchange of stabilities. In the present study the onset condition of longitudinal vortex rolls in the thermal entrance region of plane Poiseuille flow heated from below with uniform heat flux is analyzed by employing propagation theory.

2. Stability analysis

2.1. Basic flow and temperature fields

The system considered here is the thermal entrance region of plane Poiseuille flow, as shown in Fig. 1. The fluid layer is kept at uniform at T_i for $X \leqslant 0$ and heated

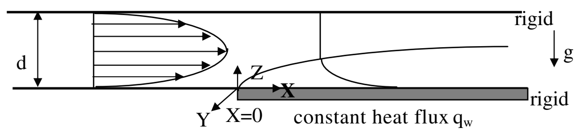

Fig. 1. Schematic diagram of system considered here.

from below with constant heat flux q_w for $X > 0$. The upper boundary is kept at constant temperature T_i. The velocity field is fully developed in the form of plane Poiseuille flow. The temperature and velocity profiles in this laminar forced convection flow of Newtonian fluid can be represented in the following dimensionless forms:

$$\overline{U}\frac{\partial\theta_0}{\partial x} = \frac{\partial^2\theta_0}{\partial z^2} + \frac{1}{Pe^2}\frac{\partial^2\theta_0}{\partial x^2}, \tag{1}$$

$$\overline{U} = 6(z - z^2), \tag{2}$$

with inlet and boundary conditions,

$$\theta_0 = 0 \quad \text{at } x = 0 \text{ and } z = 1, \tag{3a}$$

$$\frac{\partial\theta_0}{\partial z} = -1 \quad \text{at } z = 0, \tag{3b}$$

$$\theta_0 = 1 - z \quad \text{for } x \to \infty, \tag{3c}$$

where $x = X/(dPe)$, $Pe = U_{av}d/\alpha$, $z = Z/d$, $\theta_0 = k(T - T_i)/(q_w d)$ and $\overline{U} = U/U_{av}$. Here Pe denotes the Péclet number, Z the vertical distance, α the thermal diffusivity and U_{av} the average velocity. Eq. (2) would be valid with $Re < 7200$ in the present flow system under isothermal heating [4], where Re is the Reynolds number $(= U_{av}d/\nu)$.

For a large Pe, say 100, the convective heat transfer rate is much larger than the conduction one in the x-direction because the value of $1/Pe^2$ is equal to 10^{-4}. Also, with $Pe > 100$ the relation of $\Delta_T \ll d$ is kept due to $x = X/(dPe)$, where Δ_T denotes the thermal boundary-layer thickness and in the region of $Z \ll \Delta_T$ the velocity field is almost linear. Therefore, the last term in Eq. (1) is neglected in the region of small x, and $\overline{U}$ and θ_0 can be approximated as

$$\overline{U} \approx 6z. \tag{4}$$

$$\theta_0 = \frac{(1.5x)^{1/3}}{\Gamma(2/3)}\left[\exp\left(-\frac{z^3}{1.5x}\right) - \frac{z}{(1.5x)^{1/3}}\Gamma\left(2/3, \frac{z^3}{1.5x}\right)\right] = x^{1/3}\theta_0^*(\zeta) \quad \text{with} \quad \delta_T = 1.51x^{1/3}, \tag{5}$$

where $\zeta = z/x^{1/3}$ and $x < 0.05$. Here δ_T denotes the dimensionless thermal boundary-layer thickness with $\theta_0^*(\zeta)/\theta_0^*(0) = 0.01$, $\Gamma(a)$ is a gamma function, $\Gamma(a, x)[= \int_x^\infty \exp(-t)t^{a-1}\,dt]$ is an incomplete gamma function. With the above expression the Nusselt number in forced convection, $Nu(= 1/\theta_0(x, 0))$ is obtained as

$$Nu = \frac{\Gamma(2/3)}{(1.5x)^{1/3}} = 1.1829\left(RePr\frac{d}{X}\right)^{1/3}, \tag{6}$$

where the Reynolds number Re has the relation of Pe/Pr, Pr $(= \nu/\alpha)$ denotes the Prandtl number, and $RePrd/X$ is the Graetz number Gz. In general, the Leveque-type solution agrees very well with the exact solution for $Gz \geqslant 20$ [20].

2.2. Disturbance equations

By following the linear stability analysis the infinitesimal perturbation quantities $\boldsymbol{U}_1$, T_1 and P_1 are superimposed on the basic state quantities $\boldsymbol{U}_0$, T_0 and P_0 as follows:

$$(\boldsymbol{U}, T, P) = [(\boldsymbol{U}_0 + \boldsymbol{U}_1), (T_0 + T_1), (P_0 + P_1)], \tag{7}$$

where $\boldsymbol{U}$ and P denote the velocity vector and the pressure, respectively. The disturbances are usually assumed to be time-dependent, three-dimensional ones. For example, the dimensionless vertical velocity components w can be described as

$$w = w_1^*(x, y, z)\exp[\mathrm{i}(a_x x + a_y y) + \sigma\tau], \tag{8}$$

where i denotes the imaginary number, σ the temporal growth rate, and τ the dimensionless time. With the longitudinal vortex roll the amplitude function w_1^* becomes independent of spanwise distance y with $a_x = 0$ and $\sigma = 0$ while the transverse roll brings $\sigma \neq 0$ with $a_y = 0$. For a low Re and Ra with finite aspect ratio, transverse rolls can set in [21]. However, for a large Péclet number time-independent vortex rolls have been observed experimentally near the critical position [11,14–17]. In the case of isothermal heating, Kim et al.'s [7] predictions show a fairly good agreement with Lee and Hwang's [6]. In the latter work the initiated disturbances experience the temporal growth, i.e., $\sigma \neq 0$.

With $\sigma = 0$, the following dimensionless disturbance equations are obtained by invoking linear theory under the Boussinesq approximation:

$$\frac{\partial u}{\partial x} + \frac{\partial v}{\partial y} + \frac{\partial w}{\partial z} = 0, \tag{9}$$

$$\frac{1}{Pr}\left\{\overline{U}\frac{\partial u}{\partial x} + w\frac{\partial \overline{U}}{\partial z}\right\} = -\frac{1}{Pe^2}\frac{\partial p}{\partial x} + \frac{1}{Pe^2}\frac{\partial^2 u}{\partial x^2} + \frac{\partial^2 u}{\partial y^2} + \frac{\partial^2 u}{\partial z^2}, \tag{10}$$

$$\frac{1}{Pr}\left\{\overline{U}\frac{\partial v}{\partial x}\right\} = -\frac{\partial p}{\partial y} + \frac{1}{Pe^2}\frac{\partial^2 v}{\partial x^2} + \frac{\partial^2 v}{\partial y^2} + \frac{\partial^2 v}{\partial z^2}, \tag{11}$$

$$\frac{1}{Pr}\left\{\overline{U}\frac{\partial w}{\partial x}\right\} = -\frac{\partial p}{\partial z} + \frac{1}{Pe^2}\frac{\partial^2 w}{\partial x^2} + \frac{\partial^2 w}{\partial y^2} + \frac{\partial^2 w}{\partial z^2} + \theta, \tag{12}$$

$$\overline{U}\frac{\partial \theta}{\partial x} + Ra_q\left\{u\frac{\partial \theta_0}{\partial x} + w\frac{\partial \theta_0}{\partial z}\right\} = \frac{1}{Pe^2}\frac{\partial^2 \theta}{\partial x^2} + \frac{\partial^2 \theta}{\partial y^2} + \frac{\partial^2 \theta}{\partial z^2}, \tag{13}$$

with boundary conditions,

$$u = v = w = \frac{\partial \theta}{\partial z} = 0 \quad \text{at } z = 0, \tag{14a}$$

$$u = v = w = \theta = 0 \quad \text{at } z = 1, \tag{14b}$$

where $(u, v, w) = (U_1/Pe, V_1, W_1)d/\alpha$, $\theta = g\beta d^3 T_1/(\alpha\nu)$, and $p = P_1 d^2/(\alpha\nu)$. Here g denotes the gravitational acceleration, β the thermal expansion coefficient, and ν the kinematic viscosity. It should be noted that the temperature disturbance has been nondimensionalized by $\alpha\nu/(g\beta d^3)$ rather than ΔT. The most important parameter Ra_q is the Rayleigh number based on the bottom heat flux q_w, which is defined as

$$Ra_q = \frac{g\beta q_w d^4}{k\alpha\nu}. \tag{15}$$

This is sometimes called the dimensionless heat flux.

With $Pe > 100$ all the terms involving $1/Pe^2$ in Eqs. (10)–(13) are neglected like the treatment of Eq. (1). This procedure is analogous to the conventional boundary layer theory. But the resulting equations are still complicated. To examine the thermal instability of the present system the minimum value of x should be found for a given Pr and Ra_q. This means that a fastest growing instability would set in at the critical streamwise position X_c. Most of early studies on this kind of stability problem employed the assumption that disturbances would not experience variations in the streamwise direction, i.e., $\partial(\cdot)/\partial x = 0$. This model is called local stability analysis. In propagation theory this assumption is removed and it takes the streamwise propagation of disturbances into consideration.

2.3. Propagation theory

Propagation theory employed to find the dimensional critical streamwise position X_c to mark the onset of convective motion is based on the assumption that disturbances are propagated mainly within the dimensional thermal boundary-layer thickness $\Delta_T(\ll d)$ at $X_c \gg \Delta_T$. In this case the following scale analysis at $X \approx X_c$ would be valid for dimensional perturbed quantities of Eqs. (12) and (13), respectively:

$$\nu \frac{W_1}{\Delta_T^2} \sim g\beta T_1, \tag{16}$$

$$W_1 \frac{\partial T_0}{\partial Z} \sim \alpha \frac{T_1}{\Delta_T^2}. \tag{17}$$

From Eqs. (16) and (17) the following peculiar relation is obtained:

$$W_1 \sim \frac{g\beta \Delta_T^2}{\nu} T_1, \tag{18}$$

$$\frac{\partial T_0}{\partial Z} \sim \frac{\alpha\nu}{g\beta\Delta_T^4} \sim \frac{q_w}{k}\left(\frac{g\beta q_w \Delta_T^4}{k\alpha\nu}\right)^{-1} = \frac{q_w}{k} Ra_{\Delta_T}^{-1}, \tag{19}$$

where Ra_{Δ_T} is the Rayleigh number based on the length Δ_T and the bottom heat flux q_w. With increasing bottom heat flux q_w, both the critical position X_c and the corresponding Δ_T decreases while $\partial T_0/\partial Z|_{Z=0}$ increases. The order of magnitude of $k(\partial T_0/\partial Z)/q_w$ becomes equivalent to that of $Ra_{\Delta_T}^{-1}$ and Ra_{Δ_T} is assumed to reach a constant for small X_c.

The above relations are nondimensionalized as

$$\frac{w}{\delta_T^2} \sim \theta, \tag{20}$$

$$Ra_q w \frac{\partial \theta_0}{\partial z} \sim \frac{\theta}{\delta_T^2}. \tag{21}$$

This means that buoyancy-driven convection occurs due to θ and this incipient secondary flow is very weak at $x = x_c$. The resulting order of $\partial\theta_0/\partial z|_{x=x_c}$ from the above relations would be consistent with that of Eq. (19) if $Ra_q\delta_T^4$ is a constant for $\delta_T \ll 1$. In this viewpoint the basic temperature and its perturbation have been nondimensionalized having different scales. Based on the above relations, the relations of $w = \delta_T^{n+2} w^*$ and $\theta = \delta_T^n \theta^*$ can be obtained. For $n \geqslant 0$, the case of $n = 0$ gives a lower bound of Ra_q in the plot of Ra_q vs. a [22]. The case of $n < 0$ is not rational since $\theta \to \infty$ as $x \to 0$. In the present study n is set to zero because the fastest growing disturbances which give the minimum value of Ra_q are to be found. Similar treatment can be found in thermal instability analyses of various systems [23–26].

For incipient longitudinal vortex rolls we assume that steady disturbance quantities are periodic with the dimensionless spanwise wave number a. From the continuity equation of Eq. (9), the following scaling relation can be obtained:

$$u/x \sim av \sim w/\delta_T, \tag{22}$$

Since $\delta_T(\propto x^{1/3})$ or x is small in the thermal entrance region considered here, the relation of $|u| \ll |w|$ is kept but $|\partial u/\partial x|$ has the same order of magnitude as $|\partial w/\partial z|$. The scaling relation of $av \sim w/\delta_T$ is a peculiar one suggested here. It is believed that this scaling is more reasonable than others. For example, Chen and Chen [27] assumed that both v and w would have the same form. Similar scale analysis on p can be conducted through Eq. (12). Based on the above scaling, the disturbance quantities are expressed as

$$\begin{bmatrix} u(x,y,z) \\ v(x,y,z) \\ w(x,y,z) \\ p(x,y,z) \\ \theta(x,y,z) \end{bmatrix} = \begin{bmatrix} x^{4/3}u^*(\zeta) \\ (x^{1/3}/a)v^*(\zeta) \\ x^{2/3}w^*(\zeta) \\ x^{1/3}p^*(\zeta) \\ \theta^*(\zeta) \end{bmatrix} \exp(\mathrm{i}ay). \tag{23}$$

Substituting Eq. (23) into Eqs. (9)–(13) with $Pe \geqslant 100$, we can obtain the new stability equations using Eqs. (4) and (5) for small x:

$$(D^2 - a^{*2})u^* = \frac{1}{Pr}(8\zeta u^* - 2\zeta^2 Du^* + 6w^*), \tag{24}$$

$$\begin{aligned}(D^2 - a^{*2})^2 w^* = {} & a^{*2}\theta^* - \frac{1}{3}\zeta D^4 u^* + a^{*2}Du^* - \frac{1}{3}\zeta a^{*2} Du^* \\ & + \frac{1}{Pr}\left\{2\left(\frac{4}{3}u^* - \frac{1}{3}\zeta Du^* + Dw^*\right)\right. \\ & - 2\zeta\left(Du^* - \frac{1}{3}\zeta D^2 u^* + D^2 w^*\right) \\ & - 2\zeta^2\left(\frac{2}{3}Du^* - \frac{1}{3}\zeta D^3 u^* + D^3 w^*\right) \\ & \left. - 4\zeta a^{*2} w^* + 4\zeta^2 a^{*2} Dw^*\right\},\end{aligned} \tag{25}$$

$$\begin{aligned}(D^2 - a^{*2})\theta^* = {} & -2\zeta^2 D\theta^* \\ & + Ra^*\left(w^* D\theta_0^* - \frac{1}{3}\zeta u^* D\theta_0^* + \frac{1}{3}u^*\theta_0^*\right),\end{aligned} \tag{26}$$

with the following boundary conditions,

$$u^* = w^* = Dw^* = D\theta^* = 0 \quad \text{at } \zeta = 0, \tag{27a}$$

$$u^* = w^* = Dw^* = \theta^* = 0 \quad \text{as } \zeta \to \infty, \tag{27b}$$

where $D = \mathrm{d}/\mathrm{d}\zeta$, $a^* = ax^{1/3}$ and $Ra^* = Ra_q x^{4/3}$. It is noted that the above condition of $\zeta(= z/x^{1/3}) \to \infty$ is obtained as $x \to 0$. Since $Ra^* \sim Ra_{\Delta_T}$ and $a \sim 1/\delta_T$, the parameters Ra^* and a^* based on the length scaling factor $x^{1/3}$ are assumed to be eigenvalues.

Now, θ_0^*, u^*, w^* and θ^* in Eqs. (24)–(27) are functions of ζ only and their treatment like the similar transformation is possible. The principle of the exchange of stabilities is employed and the minimum value of Ra^* for a given Pr is sought. In other words, the minimum of x, i.e., x_c is found for a given Ra_q and Pr. The above whole procedure is essence of the propagation theory we have developed. The propagation theory may be called the extension of local stability analysis. If Eqs. (1) and (2) are used directly, the above transformation is not possible and mathematical difficulties will be encountered. In this case the relationship of $\delta_T \sim x^{1/3}$ is not kept and therefore the above similar transformation is not possible. Even though the present approximation produces rather simple disturbance equations, Kim et al. [7] showed that in an isothermally heated system the predictions agree well with experimental data.

In the local stability analysis x is fixed in coordinates x and z in the disturbance equations, i.e., $\partial(\cdot)/\partial x = 0$. This results in the stability equation:

$$\left(\frac{d^2}{dz^2} - a^2\right)^2 w_1 = a^2\theta, \tag{28}$$

$$Ra_q w \frac{\partial\theta_0}{\partial z} = \frac{\partial^2\theta}{\partial y^2} + \frac{\partial^2\theta}{\partial z^2}, \tag{29}$$

wherein x is the parameter. It is stated that the essential difference between local stability analysis and propagation theory comes from the different coordinate frames, i.e., (x, z) and (x, ζ), in amplitude functions. For the present system the stability equations of local stability analysis reduce to:

$$(D - a^{*2})^2 w^* = a^{*2}\theta^*, \tag{30}$$

$$(D^2 - a^{*2})\theta^* = Ra^* w^* D\theta_0, \tag{31}$$

under the following boundary conditions,

$$w^* = Dw^* = D\theta^* = 0 \quad \text{at } \zeta = 0, \tag{32a}$$

$$w^* = Dw^* = \theta^* = 0 \quad \text{at } \zeta = 1/x^{1/3}. \tag{32b}$$

2.4. Solution method

The above stability equations were solved by employing the outward shooting scheme of Chen and Chen [27]. In order to integrate these stability equations the proper values of Du^*, D^2w^*, D^3w^* and θ^* at $\zeta = 0$ were assumed for a given Pr and a^*. Since the stability equations and the boundary conditions are all homogenous, the value of D^2w^* at $\zeta = 0$ can be assigned arbitrarily and the value of the parameter Ra^* is assumed. This procedure can be understood easily by taking into account characteristics of the eigenvalue problem. After all the values at $\zeta = 0$ are provided, this eigenvalue problem can be proceeded numerically with the step size of $\Delta\zeta = 0.001$.

Integration is performed from the heated surface $\zeta = 0$ to a fictitious outer boundary with the fourth-order Runge–Kutta–Gill method. If the guessed value of Ra^*, $Du^*(0)$, $D^3w^*(0)$ and $\theta^*(0)$ are correct, u^*, w^*, Dw^* and θ^* will vanish at the upper boundary. To improve the initial guesses the Newton–Raphson iteration was used and relative errors were taken as convergence criteria. When all the relative errors were less than 10^{-10}, the outer boundary was increased by a predetermined value and the above procedure was repeated. Since the disturbances decay exponentially outside the thermal boundary layer, incremental change in Ra^* also decays fast with an increase in outer boundary depth. This behavior enables us to extrapolate the eigenvalue Ra^* to the infinite depth by the Shank transformation [28]. For example, with $Pr = 100$ the asymptotic depth was reached at $\zeta \cong 6$, which will be shown later. This means that the boundary condition of $\zeta \to \infty$ in Eq. (27) was satisfied at this vertical distance. The effect of integration depth on the critical condition was treated intensively by Chen [29], Chen et al. [30] and Kim [22]. They showed that the present extrapolation by the Shanks transformation is a good approximation method to treat the infinite outer boundary.

3. Results and discussion

The predicted values based on the above numerical scheme constitute the stability curve, as shown in Fig. 2. All these results with respect to regular longitudinal vortex flow would be valid with the assumption of $\Delta_T \ll d$. The calculated stability criteria of the minimum Ra^*, i.e., Ra_c^* are obtained and listed in Table 1. It seems

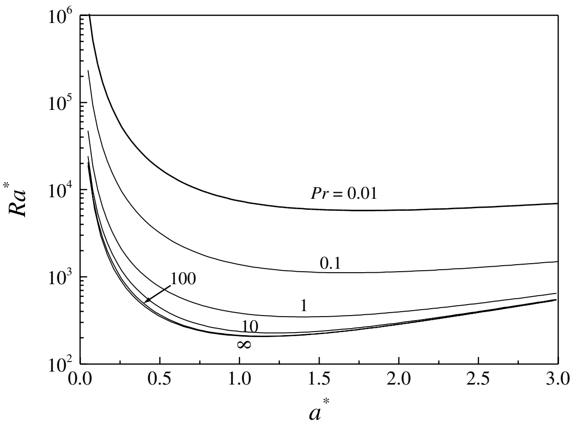

Fig. 2. Neutral stability curves for various Pr–values.

Table 1
Numerical values of Ra_c^* and a_c^* for various Pr—values

Pr	0.01	0.1	0.7	1	7	10	100	∞
Ra_c^*	5769.30	1113.10	410.11	360.41	236.62	227.93	208.86	206.17
a_c^*	1.79	1.67	1.50	1.46	1.26	1.23	1.15	1.14

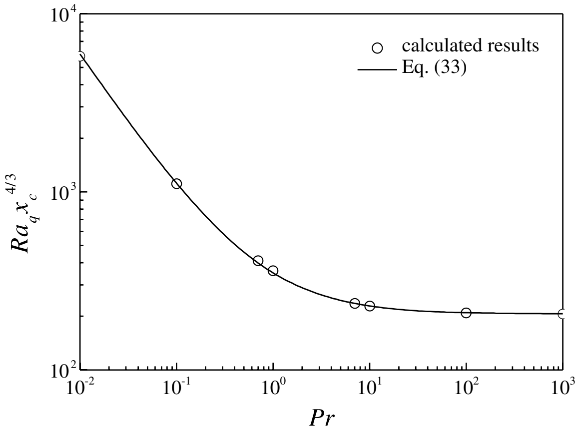

Fig. 3. Effect of Prandtl number Pr on critical condition.

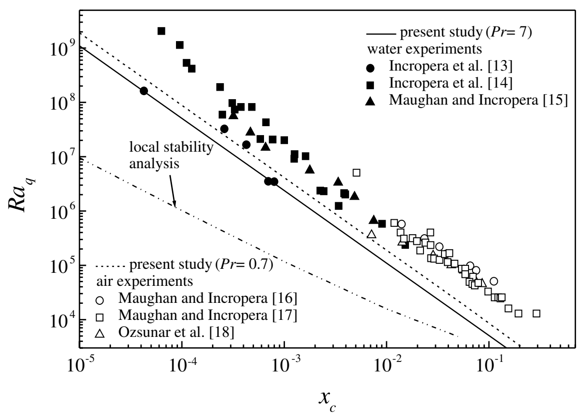

Fig. 4. Comparison of critical Rayleigh numbers with previous results.

evident that Ra_c^* increases with a decrease in Pr and the $Pr-$ effect becomes pronounced for $Pr < 1$. This means that the inertia forces make the system more stable. This trend is shown clearly in Fig. 3. As $Pr \to 0$ we can expect that the wave mode instability may prevail and the present analysis cannot be applied.

Based on Table 1, the correlation for Ra_c^* with Pr is obtained first. And then, by using the relation of $Ra^* = Ra_q x^{4/3}$ and $x = X/(d\,Re\,Pr)$, the dimensional critical position X_c for a given Ra_q can be represented by the following correlation:

$$x_c = \frac{X_c/d}{PrRe} = \left[\frac{206.17}{Ra_q}\left(1 + \frac{0.7}{Pr^{0.8}}\right)\right]^{3/4}, \tag{33}$$

which represents the predictions very well with the error bound of 3% for $Pr \geqslant 0.01$, $Pe(= PrRe) \geqslant 100$ and $x_c(= X_c/(dPe)) \leqslant 0.05$. Our analysis is based on the assumption that $Re < 7200$ and $Pe > 100$. So, it should be kept in mind that the present analysis is limited to the system of $Pr > 0.013(= 100/7200)$. The dimensionless critical position x_c to mark the onset of longitudinal vortex rolls becomes smaller with an increase in Ra_q and Pr. For a given Re and Ra_q the dimensional position X_c becomes larger with an increase in Pr. The Reynolds number delays the onset of longitudinal vortex rolls.

Incropera and his colleagues [13–18] reported their experimental data of thermal instability that the onset of secondary flow precedes appreciable heat transfer measurement. In Fig. 4, their data of water and air are compared with the present critical conditions (Table 1):

$$x_c = 60.16 Ra_q^{-3/4} \quad \text{and}$$
$$a_c = 0.319 Ra_q^{1/4} \quad \text{for } Pr = 7, \tag{34a}$$

$$x_c = 87.18 Ra_q^{-3/4} \quad \text{and}$$
$$a_c = 0.323 Ra_q^{1/4} \quad \text{for } Pr = 0.7. \tag{34b}$$

It is shown that the present predictions from propagation theory provide lower bounds in the whole experimental range and the difference between water and air is not so large. For $Ra_q > 10^5$ the predictions from the local stability analysis are about two orders of magnitude lower than those from propagation theory but the difference becomes smaller as Ra_q decreases. Eq. (34a) is comparable with the numerical results of Maughan and Incropera [15]. Secondary flow is possible for $Ra_q \geqslant 1296$. For $Ra_q = 1296$ the flow and temperature fields are fully developed with $a_c = 2.55$.

At experimental environments the boundary imperfection exist and therefore, the experimental data scatter rather widely, as shown in Fig. 4. But the trend supports the present predictions to a certain degree. The predicted a_c for $Pr = 7$ is compared with the experimental data of water in Fig. 5. The present critical wave number shows good agreement with the last four data points of Maughan and Incropera [15]. For $Ra_q \leqslant 10^7$, less than 10 vortex pairs were observed in experiments of the aspect ratio of about 10. The large discrepancy of the first two points from predictions may be attributed to the side wall effects. In both laminar forced convection [31] and

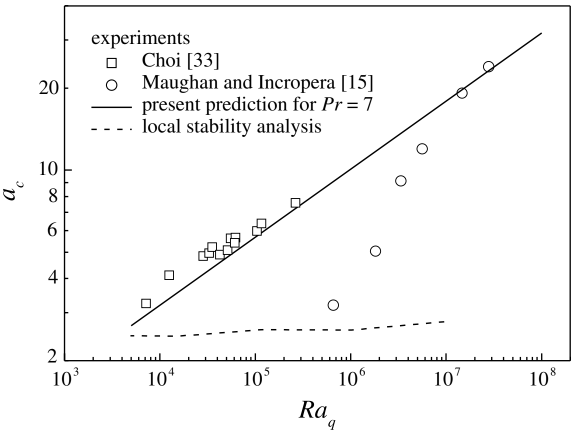

Fig. 5. Comparison of predicted critical wave numbers with available experimental ones for water.

Rayleigh–Bénard convection [32] of low Ra, patterns of incipient natural convection is strongly influenced by the side wall effects. The present system leads to the plane Couette flow for small x. For this flow system of the upper free boundary, Choi [33] conducted water experiments of uniform heat flux with the aspect ratio of about 50 and his experimental data points agree well with the present predictions from propagation theory, as shown in Fig. 5. The related stability analysis is summarized in the work of Choi and Kim [19]. It is stated that the present work complements their work.

The above reasoning supports, to a certain degree, that propagation theory provides rather reasonable critical conditions to mark secondary flow in form of regular longitudinal rolls. Therefore, their amplitude functions need to be examined in detail. At the critical conditions illustrated above, the amplitude functions of w^* and θ^* are featured in Fig. 6, wherein the quantities have been normalized by the corresponding maximum magnitude $w^*_{\max}$ and $\theta^*_{\max}$. It is seen that incipient temperature disturbances are confined mainly within the dimensionless thermal boundary-layer thickness $\delta_T(= 1.51x^{1/3})$ but velocity disturbances are driven more upward over the thermal boundary-layer thickness with increasing Pr. As Pr decreases, the vertical position showing $w^*_{\max}$, i.e., $\zeta|_{w^*_{\max}}$ moves to the heated surfaces. Also, the dimensionless hydrodynamical boundary-layer thickness $\zeta|_{w^*_{0.01}}$ is larger than the thermal one $\zeta|_{\theta^*_{0.01}}$, where the boundary-layer thickness is defined as the depth to exhibit the normalized magnitude of 0.01. This means that the secondary motion of vortex rolls is driven thermally.

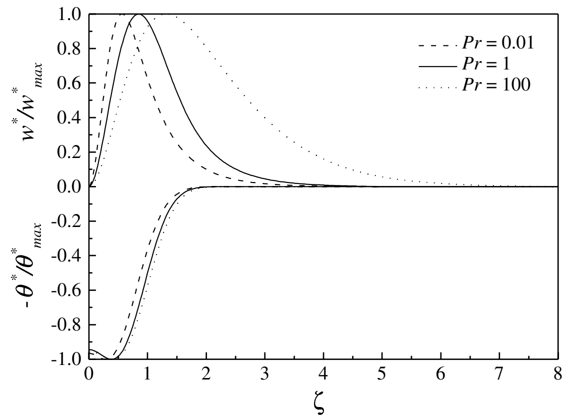

Fig. 6. Normalized amplitude profiles of disturbances.

4. Conclusion

The critical condition of the onset of secondary flow in form of regular longitudinal vortex rolls in the thermal entrance region of plane Poiseuille flow heated uniformly from below has been analyzed based on propagation theory. It is interesting that the onset position X_c moves downstream with an increase in Prandtl number and Reynolds number. The present predictions agree reasonably well with the existing experimental data of water and air. It may be stated that our propagation theory is a useful tool to analyze the buoyancy-driven instabilities in laminar forced convection flow.

Acknowledgements

This work was partially supported by LG Chemical Ltd., Seoul and T.J. Chung acknowledges the financial support from the Brain Korea 21 Project of the Ministry of Education.

References

[1] H. Bénard, Les tourbillons celluaries dans une nappe liquide transportant de la chaleur par convection en regime permanent, Annales de Chimie et de Physique 23 (1901) 62–144.
[2] L. Rayleigh, On convection current in a horizontal layer of fluid when the higher temperature is on the under side, Philosophical Magazine 32 (1916) 529–546.
[3] K.-C. Chiu, F. Rosenberger, Mixed convection between horizontal plates-I. Entrance effects, International Journal of Heat and Mass Transfer 30 (1987) 1645–1654.
[4] K.S. Gage, W.H. Reid, The stability of thermally stratified plane Poiseuille flow, Journal of Fluid Mechanics 33 (1968) 21–32.
[5] G.J. Hwang, K.C. Cheng, Convective instability in the thermal entrance region of a horizontal parallel-plate channel heated from below, Transactions of ASME: Journal of Heat Transfer 95 (1973) 72–77.
[6] F.S. Lee, G.J. Hwang, Transient analysis on the onset of thermal instability in the thermal entrance region of

horizontal parallel plate channel, Transactions of ASME: Journal of Heat Transfer 113 (1991) 363–370.
[7] M.C. Kim, J.S. Baik, I.G. Hwang, D.-Y. Yoon, C.K. Choi, Buoyancy-driven convection in plane Poiseuille flow, Chemical Engineering Science 54 (1999) 619–632.
[8] G.J. Hwang, C.L. Liu, An experimental study of convective instability in the thermal entrance region of a horizontal parallel-plate channel heated from below, Canadian Journal of Chemical Engineering 54 (1976) 521–525.
[9] Y. Kamotani, S. Ostrach, Effect of thermal instability on thermally developing laminar channel flow, Transactions of ASME: Journal of Heat Transfer 98 (1976) 62–66.
[10] Y. Kamotani, S. Ostrach, H. Miao, Convective heat transfer augmentation in thermal entrance region by means of thermal instability, Transactions of ASME: Journal of Heat Transfer 101 (1979) 222–226.
[11] D.G. Osborne, F.P. Incropera, Laminar, mixed convection heat transfer for flow between horizontal parallel plates with asymmetric heating, International Journal of Heat and Mass Transfer 28 (1985) 207–217.
[12] F.P. Incropera, J.A. Schutt, Numerical simulation of laminar mixed convection in the entrance region of horizontal rectangular ducts, Numerical Heat Transfer 8 (1985) 707–729.
[13] F.P. Incropera, A.L. Knox, J.A. Schutt, Onset of thermally driven secondary flow in horizontal rectangular duct, in: Proceedings of the Eighth International Heat Transfer Conference, vol. 3, Hemisphere, Washington DC, 1986, pp. 1395–1400.
[14] F.P. Incropera, A.L. Knox, J.R. Maughan, Mixed-convection flow and heat transfer in the entry region of a horizontal rectangular duct, Transactions of ASME: Journal of Heat Transfer 109 (1987) 434–439.
[15] J.R. Maughan, F.P. Incropera, Secondary flow in horizontal channels heated from below, Experiments in Fluids 5 (1987) 334–343.
[16] J.R. Maughan, F.P. Incropera, Experiments on mixed convection heat transfer for airflow in a horizontal and inclined channel, International Journal of Heat and Mass Transfer 30 (1987) 1307–1318.
[17] J.R. Maughan, F.P. Incropera, Regions of heat transfer enhancement for laminar mixed convection in a parallel plate channel, International Journal of Heat and Mass Transfer 33 (1990) 555–570.
[18] A. Ozsunar, S. Baskaya, M. Sivrioglu, Experimental investigation of mixed convection heat transfer in an horizontal and inclined rectangular channel, Heat and Mass Transfer 38 (2002) 271–278.
[19] C.K. Choi, M.C. Kim, Buoyancy effects in plane Couette flow heated uniformly from below, in: Proceedings of the Tenth International Heat Transfer Conference, vol. 5, Brighton, UK, 1994, pp. 453–458.
[20] L.C. Burmeister, Convective Heat Transfer, second ed., Wiley, New York, 1993, p. 143.
[21] X. Nicolas, J.-M. Luijkx, J.-K. Platten, Linear stability of mixed convection flows in horizontal rectangular channels of finite transversal extension heated from below, International Journal of Heat and Mass Transfer 43 (2000) 589–610.
[22] M.C. Kim, The onset of natural convection and heat transfer correlations in systems experiencing thermal boundary layer characteristics, PhD. thesis, Seoul National University, Seoul, Korea, 1992.
[23] I.G. Hwang, C.K. Choi, An analysis of the onset of compositional convection in a binary melt solidified from below, Journal of Crystal Growth 162 (1986) 182–189.
[24] K.H. Kang, C.K. Choi, A theoretical analysis of the onset of surface-tension-driven convection in a horizontal liquid layer cooled suddenly from above, Physics of Fluids 9 (1997) 7–15.
[25] M.C. Kim, K.H. Choi, C.K. Choi, The onset of thermal convection in an initially, stably stratified fluid layer, International Journal of Heat and Mass Transfer 42 (1999) 4253–4258.
[26] D.H. Lee, D.Y. Yoon, C.K. Choi, The onset of vortex instability in laminar natural convection flow over an inclined plate embedded in a porous medium, International Journal of Heat and Mass Transfer 43 (2000) 2895–2908.
[27] K. Chen, M.M. Chen, Thermal instability of forced convection boundary layers, Transactions of ASME: Journal of Heat Transfer 106 (1984) 284–289.
[28] O.T. Hanna, O.C. Sandall, Computational method in chemical engineering, Prentice Hall, Englewoood Cliffs, NJ, 1995, pp. 84–85.
[29] K. Chen, Thermal instability of wedge flows, PhD. thesis, University of Illinois, Urbana-Champaign, IL, 1981.
[30] K. Chen, M.M. Chen, C.W. Sohn, Thermal instability of two-dimensional stagnant-point boundary layers, Journal of Fluid Mechanics 132 (1983) 49–63.
[31] M.Y. Chang, T.F. Lin, Experimental study of aspect ratio effects on longitudinal vortex flow in mixed convection of air in a horizontal rectangular duct, International Journal of Heat and Mass Transfer 41 (1998) 719–733.
[32] C.W. Meyer, G. Ahlers, D.S. Cannell, Stochastic influences on pattern formation in Rayleigh–Bénard convection: ramping experiments, Physical Review A 44 (1991) 2514–2537.
[33] C.K. Choi, Thermal convection in the liquid film of a stratified gas/liquid flow, Ph.D. thesis, Clarkson University, Potsdam, NY, 1976.